

Numerical Analysis of a Cold Air Distribution System

Liyang Zhu Rui Li Dongzhao Yuan
 Postgraduate Professor Postgraduate
 Beijing Institute of Civil Engineering and Architecture
 Beijing, China, 100044
 zhuliyang518@163.com

Abstract: Cold air distribution systems may reduce the operating energy consumption of air-conditioned air supply system and improve the outside air volume percentages and indoor air quality. However, indoor temperature patterns and velocity field are easily non-uniform so that residents usually feel uncomfortable. The distribution of indoor airflow by cold air distribution is researched in this paper. We study indoor air distribution under different low temperature air supply conditions by numerical simulation. The simulated results agree well with the experiments.

Key words: Cold air distribution system; Numerical simulation; Velocity field; Temperature field

1. INTRODUCTION

Cold air distribution system has many characters such as low temperature and big temperature differential of supplying air, low relative humidity indoors, and high dry bulb temperature, saving energy and being economic. However, the system makes indoor temperature and velocity field non-uniform easily. If air-supply velocity is lower and cold draft blow can't reach the design request, it may form subsidence of cold air so that human being will feel discomfort. And supply air of lower temperature enters the air-conditioned space directly; it can make local humidity too low and indoor temperature non-uniform to impact the heat comfort. Supply air temperature, which isn't being specially handled, may lower than the dew point temperature in air-conditioned space that can lead to air atomizing. This state is particularly obvious when the air-conditioned equipment start and it can generate water-condensing and water-drip on air outlets, which can damage indoor environment. Therefore, numerical simulation of air-supply characteristics and

prediction of indoor air distribution of cold air distribution system are important to optimize air distribution in air-conditioned space and design and applications.

This article studies indoor cold air distribution under different conditions by numerical simulation, and the simulation results are consistent with the experimental research.

2. CHARACTERISTICS OF COLD AIR DISTRIBUTION SYSTEM

Cold air distribution has a lot of advantages^[1]: heat comfort and the air-supplying quality improved by lower indoor relative humidity to improving indoor air quality; saving energy cost and energy consumption of supply fan being reduced by 30~40%.

High temperature differential is used during air supplying, and the temperature differential is usually 13~20°C, while the conventional mode is 8~10°C. Meanwhile, the size of ducts and equipment in such systems are reduced, as well as the first cost. The building space is reduced and the construction cost is saved, thus the storey height of building is reduced.

As a result, cold air distribution system is a kind of energy-saving system and has highly economic and social benefits.

3. PHYSICAL MODELS

3.1 Physical Models of Air-conditioned Space

This subject took an experimental air-conditioned room as a simulative object. The size of the room is 7200mm×5600mm×3200mm (length×width×height). It has two steel sashes in the south which size are 2350mm×1750mm (width ×

height), and the rest three walls are all interior ones. The adjacent rooms are not air-conditioned space. The ceiling air-outlet was 2.8m high above which the air distribution was not influenced greatly, so the physical model's height was 2.8m.

Here two kinds of air-outlets made of aluminum alloy were used—ceiling air-outlets which were rectangular air distributor and wall air supply which were double louver air-outlets. Where return air intake-linear grille and wall air-outlets laid were interior walls. The models built were shown as Fig. 1 (wall air-outlet) and Fig.2 (ceiling air-outlet). In the room working men was 3, desks 3, cupboard 1 and headlights 4.

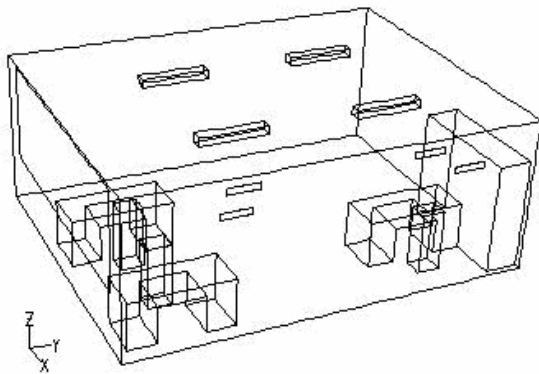


Fig. 1 physical model of wall air supply

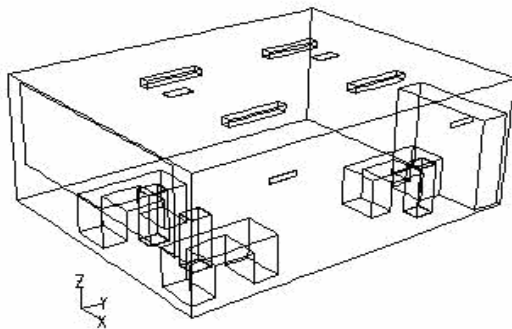


Fig. 2 physical model of ceiling air-supply

Note: X forward was east; Y forward north and Z forward the room height.

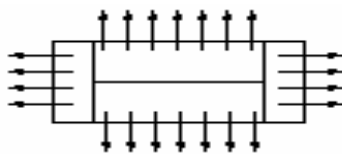


Fig.3 the model of rectangular air distributor

3.2 The Models of Air-outlets

The models of outlets were shown as Fig.3 and Fig.4. To assure the direction of air-current possibly close to practice, the rectangular air distributors, which used basic model, adopted 4 simple apertures

in different directions, and the degree of the direction of air flow and the ceiling was 45° or 30° . The air rate was distributed depended on the proportion between area of efflux and the actual one. The air supply by double louver air-outlets using basic model was horizontally along with ceiling.

4. MATHEMATICAL MODELS AND BOUNDARY CONDITIONS

4.1 Mathematical Models

This paper simulated three-dimensional incompressible turbulence of indoor air by turbulence model [3]. To simplify the issue, the models were assumed as follows:

1) The indoor air was incompressible, invariable property, steady-state flow and coincidence with the

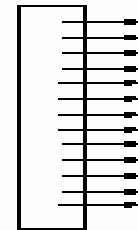


Fig.4 the model of double louver air-outlet

basic assumption of Boussinesq.

- 2) Heat-transfer in walls was equable and it was considered as steady-state.
- 3) Air leakage was without consideration. The door and windows were assumed to be closed when air supplying and their sealing performance was good.
- 4) Glass scattering to solar radiation and the impact of interior heat-transfer surfaces were not considered.
- 5) There was not internal heat source indoors.

The turbulence model, considering the influence of buoyant force, adopted two-equation model with high-Reynolds against little air-supply quantity and low air velocity in air-conditioned space, and simulative computation was combination with the wall-function method.

Continuity equation

$$\frac{\partial (\rho u_i)}{\partial x_i} = 0 \tag{1}$$

Momentum conservation equation

$$\frac{\partial(\rho u_i)}{\partial t} + \frac{\partial(\rho u_j u_j)}{\partial x_j} = \frac{\partial p}{\partial x_j} \left[(\mu + \mu_t) \left(\frac{\partial u_i}{\partial x_j} + \frac{\partial u_j}{\partial x_i} \right) \right] - \rho \beta (T - T_\infty) g_i \quad (2)$$

Turbulence energy equation (*k* equation)

$$\frac{\partial(\rho k)}{\partial t} + \frac{\partial(\rho u_j k)}{\partial x_j} = \frac{\partial}{\partial x_j} \left[\left(\mu + \frac{\mu_t}{\sigma_k} \right) \frac{\partial k}{\partial x_j} \right] + \mu_t \frac{\partial u_i}{\partial x_j} \left(\frac{\partial u_i}{\partial x_j} + \frac{\partial u_j}{\partial x_i} \right) - \rho \varepsilon \quad (3)$$

Turbulence energy dissipation equation (*ε* equation)

$$\frac{\partial(\rho \varepsilon)}{\partial t} + \frac{\partial(\rho u_j \varepsilon)}{\partial x_j} = \frac{\partial}{\partial x_j} \left[\left(\mu + \frac{\mu_t}{c_\varepsilon} \right) \frac{\partial \varepsilon}{\partial x_j} \right] + \frac{\varepsilon}{k} c_{1\mu_t} \frac{\partial u_i}{\partial x_j} \left(\frac{\partial u_i}{\partial x_j} + \frac{\partial u_j}{\partial x_i} \right) - c_{2\rho} \frac{\varepsilon^2}{k} \quad (4)$$

Energy conservation equation

$$\frac{\partial \rho T}{\partial t} + \frac{\partial(\rho u_j T)}{\partial x_j} = \frac{\partial p}{\partial x_j} \left[\left(\frac{k}{c_p} + \frac{\mu_t}{\sigma_t} \right) \frac{\partial T}{\partial x_j} \right] + S_T \quad (5)$$

In the equations, $c_1, c_2, c_p, \sigma_\varepsilon, \sigma_t,$

σ_c were all constants. Their values were shown as Tab.1 according to B.E.Launsder's and D.B.Spalding's recommendations.

Tab.1 Empirical constants of *k* – *ε* model

c_u	c_1	c_2	σ_k	σ_ε	σ_t
0.09	1.44	1.92	1.0	1.3	0.9~1.0

Tab.2 Entrance boundary in simulative condition

Conditions	Mode	Diffuser size mm× mm	<i>u</i> m/s	<i>Q</i> m ³ /s
1	Ceiling supply and wall return	620×320	1.5	0.304
2	Wall supply and return	700×160	2.0	0.304

4.2 Boundary Conditions

At the air-inlets the boundary velocity *u* (m/s) and temperature *t* () were shown as Tab.2. *k* was a percentage of average kinetic energy at the air-inlets,

usually 0.5~1.5%. $\varepsilon = \frac{c^{3/4} k_p^{3/4}}{k y_p}$, it was determined

by the relations between turbulence Reynolds at air-inlets and turbulence characteristic length. In this paper, *k*=0.04 (turbulence kinetic energy), and

$\varepsilon=0.008$ (turbulence dissipation).

The Outlet boundary was treated with coordinate local unilateralization. It was assumed that the nodes at exit section didn't influence the first interior node, and so the influence coefficient result from boundary node influencing interior nodes. That is, information at exit section played no role on interior nodes computation, and exit boundary conditions were not considered.

For the solid boundary, the air velocity is zero paralleled with walls, as well as that vertical to walls, for $\frac{\partial u}{\partial x} = \frac{\partial v}{\partial y} = 0$ near walls and $\frac{\partial w}{\partial z} = 0$ according to continuity equation.

The spread coefficient of *k* is zero.

The dissipation of turbulence kinetic energy may be calculated as Equation (6):

$$\varepsilon = \frac{c^{3/4} k_p^{3/4}}{k y_p} \quad (6)$$

The fixed surfaces such as ceiling, walls all-around, floor and desks were not gliding plane; the windows were the first boundary condition and its temperature was 36 , the external wall—the south wall was also the first boundary condition and its temperature 34 , the temperature of the rest walls was 29 .

5. NUMERICAL COMPUTATION

The computational meshes were portioned with rectangular coordinate system, and the step-size of the main meshes was 0.15m on the directions of three coordinate axes. The meshes were encrypted at human bodies, objects around, air-inlets and air-outlets.

The numerical solution procedure about the problems of flow and heat transfer was as follows: firstly, the solved area was dispersed and meshed; secondly, variable-values were defined on mesh nodes, and algebraic equation systems were got after dispersing control equations; finally, the numerical solution was obtained by solving the equations.

6. NUMERICAL SIMULATION RESULTS

Eight sections were selected in the simulation,

which were $x=1.0\text{m}$; 2.8m ; 3.6m , $y=0.7\text{m}$; 1.9m ; 3.1m , $z=1.2\text{m}$; 1.8m .

6.1 Ceiling Air Supply Condition

Fig.5 to Fig.7 shows the temperature field of typical sections. Fig.8 and fig.9 shows the velocity field of typical sections.

It could be seen from Fig.5 to Fig.9 that air supply quantity was small, as well as vortex and velocity change with cold air. Because of gravitational impact on the jet, it was easily to generate cold fallout which made the angle of flare small. The cold jet in temperature field formed temperature fallout easily and the temperature in workplace was low. The area having higher temperature in velocity field was small and the velocity uniformity was good, and the air fallout was obvious under the air-outlets for the faster velocity; meanwhile, the velocity near the floor and ceiling was apparently lower and the gradient was also smaller. It was mainly because the air supply quantity was small and cold fallout was generated with cold air.

6.2 Wall Air Supply Condition

Fig.10 to Fig.13 shows the temperature field of typical sections. Fig.14 and fig.15 shows the velocity field of typical sections.

It could be concluded from Fig.10 to Fig.15 that at section $x=2.8\text{m}$ the lower temperature area enlarged in the southern floor and the higher one in the upper and north of the room reduced; at section $x=3.6\text{m}$ the small area of relatively lower appeared underneath the room and the higher temperature one expanded. By section $z=1.2\text{m}$, the higher one was yet at the south-east corner. In the velocity field, however, the cold jet in the south was shorter than the north one, and the retention area of the cold air was larger.

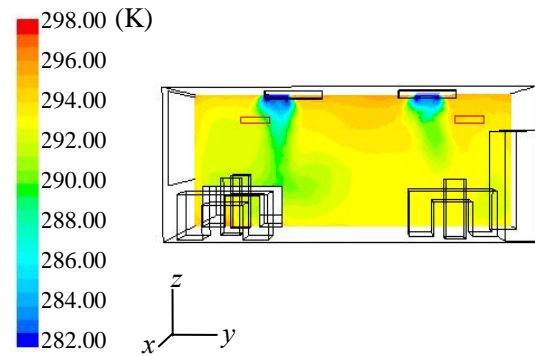


Fig.5 Section $x=2.8$

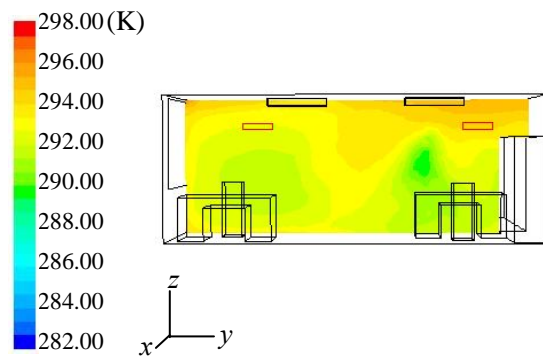


Fig.6 Section $x=3.6$

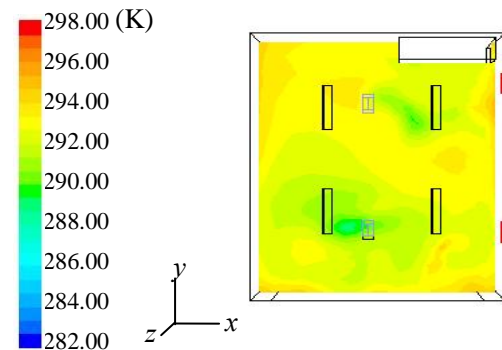


Fig.7 Section $z=1.2$

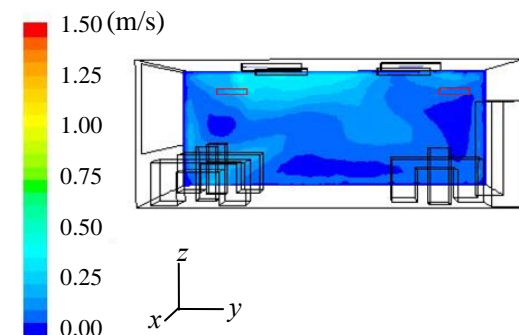


Fig.8 Section $x=1.0$

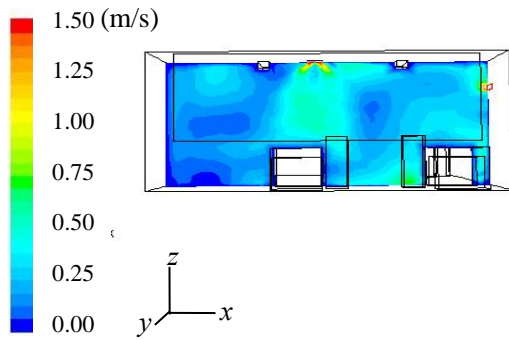


Fig.9 Section y=1.9

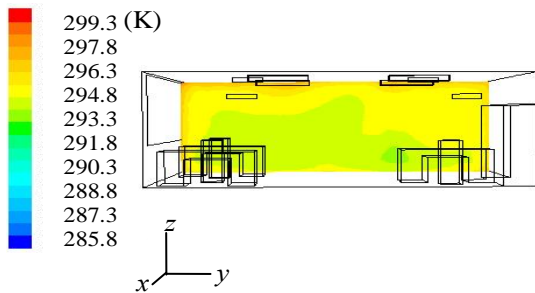


Fig.10 Section x=1.0

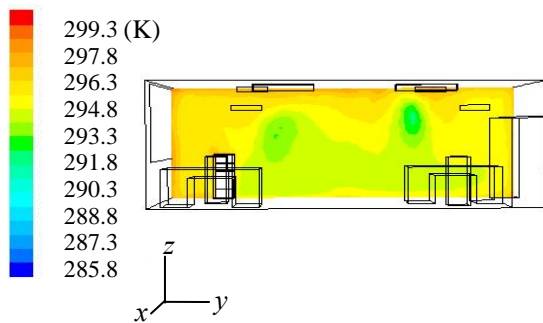


Fig.11 Section x=2.8

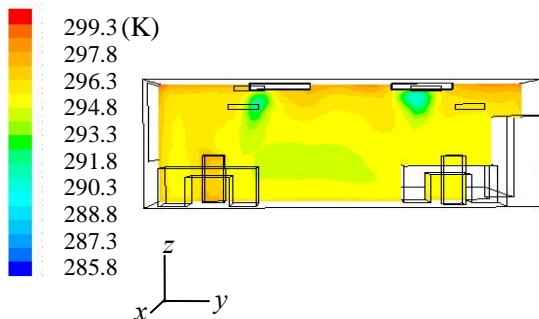


Fig.12 Section x=3.6

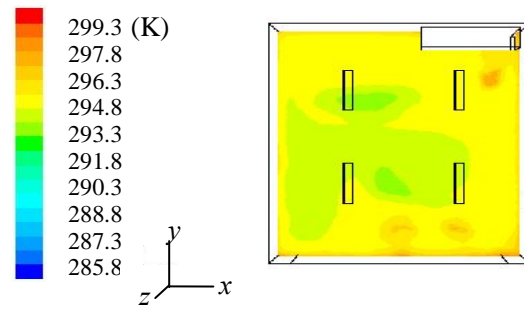


Fig.13 Section z=1.2

7. THE VALIDITY OF NUMERICAL SIMULATION RESULTS

To verify the numerical simulation results, the test was done. In the experiment, there were 9 measuring points, which were $x=1.0\text{m}$, 2.8m , 4.6m

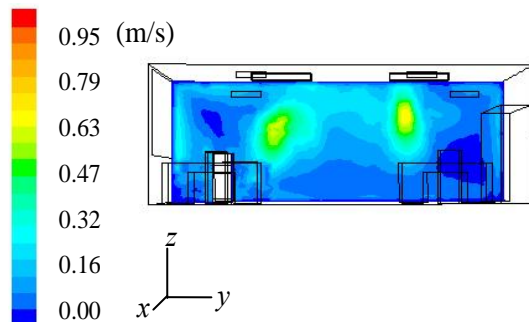


Fig.14 Section x=2.8

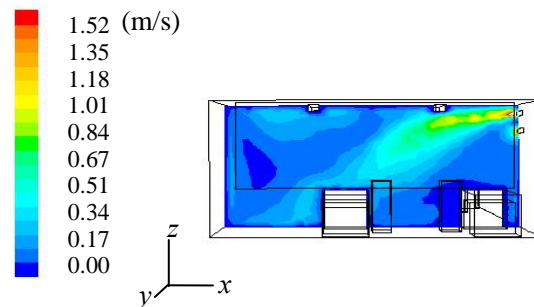


Fig.15 Section y=1.9

and $y=0.7\text{m}$, 1.9m , 3.1m and $z=1.2\text{m}$, 2.8m . The thermostatic multi-anemometer was used to measure the velocity and temperature of air in the air-conditioned room. The measured results were compared with those of the simulation.

By analysis the maximum of the temperature absolute deviation was 2.1 and the relative one was 9.1% and the average deviation of them both were 5.2%, 7.1%, which indicated that the temperature field was simulated reasonable; meanwhile, the

maximum of the velocity absolute deviation was 0.08m/s and the relative one was larger, but the air velocity was small and less than 0.3m/s, so the simulation of velocity field was also reasonable.

8. CONCLUSIONS

Based on analysis above, the conclusions as follows:

1) Human beings easily feel cold-air blowing in cold air-conditioned room, so the air-current was essentially researched and acknowledged. The Fluent software was used to simulate the air flow in an air-conditioned room with cold air supply, and it is reasonable compared with the experimental results.

2) The air fallout is easily generated and the air detention area and eddy current are existent. The same case occurs with both ceiling and wall air supply.

3) According to the comparison analysis between numerical simulation and experiment, the mathematical model and boundary conditions are considered correct and reasonable, which can be used to analyze indoor heat and humidity environment with cold air distribution system in different conditions.

REFERENCES

- [1] Written by Allan T.kirpatrick and James S.Elleson. Translated by Xunchang WANG .Cold Air Distribution System Design Guide[M]. China Architecture & Building Press. 1999.12.(In Chinese)
- [2] Deyuan CAI, Yanzheng GUAN, Yanlin ZENG. Evaluation of Performance of Cold Air Distribution Diffuser[J]. Journal of Southeast Jiaotong University, 2002 (1): 85-89.
- [3] Guangfa TANG etc. Numerical Computation and Model Experiment on indoor airflow [M]. Changsha: Hunan University Press, 1989. (In Chinese)
- [4] Wenquan TAO. Numerical Heat Transfer (Second Edition) [M]. Xi'an Jiaotong University Press, 2002.5. (In Chinese)
- [5] Bin ZHAO, Xianting LI, Qisen YAN. Review of Air Supply Opening Models in Numerical Simulation of Indoor Air Flow [J]. HV&AC. 2000, 30(5):33-37. (In Chinese)